

Anomalous exchange interactions in III-V dilute magnetic semiconductors

Mark van Schilfgaarde and O. N. Mryasov
 Sandia National Laboratories, Livermore, California, 94551
 (Received 15 February 2001; published 31 May 2001)

Based on local-density functional calculations, we study the exchange interactions between magnetic dopants Cr, Mn, and Fe in the III-V compounds GaAs, GaN, and AlN. We show the magnetic exchange interactions deviate strongly in behavior expected from simple models, and may explain the observed maximum in critical temperature with impurity concentration. Additionally the magnetism is responsible for a strong, short-range attraction between the magnetic dopants, thus creating an anomalous effective alloy hamiltonian. This suggests that the impurities may aggregate into small nanoclusters of a few magnetic atoms.

DOI: 10.1103/PhysRevB.63.233205

PACS number(s): 75.50.Pp, 75.30.Et, 75.50.Dd

In recent years, metallic magnetic superlattices have enjoyed considerable success. They are now used commercially in magnetic read heads, and there is great interest in using them or magnetic superlattices with nonmagnetic spacers as electronic devices. Recently, it was shown that the $\text{Mn}_x\text{Ga}_{1-x}\text{As}$ alloy, for $x < 0.10$, undergoes a spontaneous transition to a ferromagnetic (FM) state at temperatures below 100 K.¹ The discovery ferromagnetism *within* a semiconductor has spawned a great deal of recent interest in understanding the magnetic behavior, both fundamentally and with a view toward using the magnetic degrees of freedom in novel devices, for example, as spin filters or in magnetically controllable electronics. It was quickly recognized that Mn behaves differently in the III-V compounds such as GaAs (substituting for the cation) than when alloyed in the conventional II-VI compounds such as ZnTe, because it acts both as a magnetic element and as a p -type dopant, which at concentrations of $\sim 5\%$, renders the host metallic.

This report presents two independent findings for III-V compounds GaAs, GaN, and AlN doped with 1 to 5 % concentrations of magnetic transition-metal (TM) elements Mn, Cr, and Fe, based on the local spin-density approximation. First, the exchange interactions are anomalous and behave quite differently from simple models such as a Ruderman-Kittel-Kasuya-Yosida (RKKY)-like theory.^{2,3} Most strikingly, the effective pair interactions *decrease with increasing dopant concentration*; moreover, a pairwise description itself is not adequate. We show that the transition metal (TM) d states generate deep levels that strongly perturbs the host band structure—in particular, the states at the Fermi level. Second, the magnetism is responsible for an anomalously strong and attractive alloy Hamiltonian (coupling between Mn and the semiconductor cation nuclei), thereby inducing a strong driving force for the Mn to group together in small nanoclusters of a few atoms. (Whether the clustering actually takes place depends on kinetic considerations, which we do not address here.)

We consider small molecular clusters of cation-substituted TM impurities embedded in a III-V host. For computational convenience, we employ 216-atom supercells of the zinc-blende structure here throughout except where specified. A supercell with one defect thus corresponds to $1/108 \approx 1\%$ doping. Calculations were made self consistent in the atomic spheres approximation.⁴ They were checked in

a few cases against more accurate full-potential calculations, and found to be adequate for the present purposes. The tetrahedron method with Blöchl weights⁵ and 27 k points was used for Brillouin zone integrals, which resulted in a convergence to a precision of ~ 5 meV.

Let us consider first an isolated TM impurity. The TM d states split into a triply degenerate t_{2g} and a doubly degenerate e_g level for each spin. In GaN the calculated levels sit at 1.44 and 0.22 eV, respectively, above the valence band maximum (VBM). Their width is ~ 0.1 eV, establishing that a 216-atom cell reasonably describes the dilute limit. The levels are spin split by about ~ 2 eV; thus the minority states are resonant in the conduction band because the local-density approximation (LDA) gap is ~ 2 eV.

In GaAs, the valence band lies higher owing to the shallower anion p state, and the calculated majority Mn t_{2g} state now falls to VBM+0.08 eV, in good agreement with an experimentally observed level for Mn in GaAs.² That the theory and experiment agree in this case suggests that the LSDA adequately describes the electronic structure of such compounds—a significant point, in light of its tendency to underestimate the on-site Mn spin splitting in somewhat similar circumstances.⁶ Figure 1 shows the systematic evolution of the t_{2g} level as a function of host material and impurity atomic number Z . The levels sink with increasing Z because the impurity potential deepens.

The majority t_{2g} level is doubly occupied in the case of Mn and fully occupied in the case of Fe. In all cases (AlN, GaN, GaAs), the self-consistent magnetic moments are integral values: $3\mu_B$ in Cr, $4\mu_B$ in Mn, and $5\mu_B$ in Fe. These data are consistent with the accepted picture that Mn contributes 5 d electrons+one hole, doping the host p type, while Fe contributes 5 d electrons without doping. However, the hole differs markedly from the usual variety, as can be seen

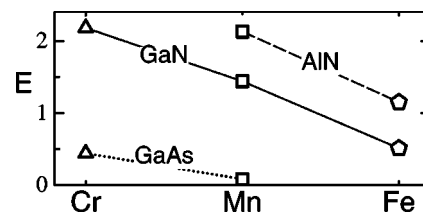


FIG. 1. Calculated position of Cr, Mn, and Fe the majority t_{2g} levels relative to the valence-band maximum, in eV.

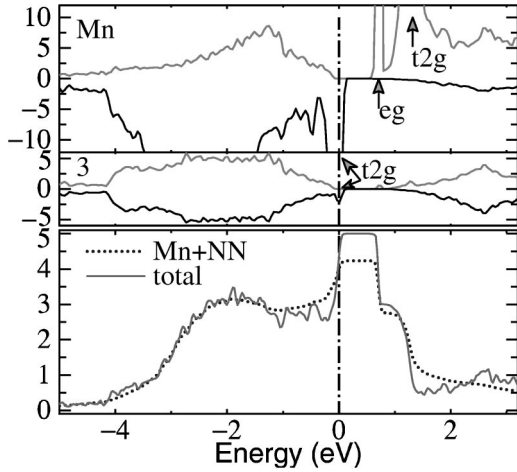


FIG. 2. DOS $N(E)$ of Mn impurity in 216-atom GaAs supercell. Dot-dashed line delineates Fermi level. Top panel: partial DOS in sphere centered at Mn; second panel: partial DOS centered at the third-neighbor As sphere. Light and dark lines are majority— and minority—spin channels, respectively. Peaks for majority t_{2g} and minority t_{2g} and e_g states are labeled. Bottom panel: total energy-integrated spin DOS $I(E)$ and the partial contribution to I from the Mn site and the first shell of As neighbors (dotted line). At E_F the DOS (slope of I) are approximately equally apportioned into the local and extended parts.

in Fig. 2. The top panels show the self-consistent spin- and energy-resolved density of states (DOS), decomposed into partial waves centered at Mn and at the third-neighbor As site. Both minority levels (t_{2g} and e_g) are marked, as is the majority t_{2g} . Comparing the areas of majority t_{2g} peak ($E = E_F = 0$) at the Mn to the third-neighbor As site, is evident that the t_{2g} state is strongly localized around the Mn site. This is quantified in the bottom panel, which shows the total integrated spin DOS, $I(E) = \int_{-\infty}^E N^\uparrow(\epsilon) - N^\downarrow(\epsilon) d\epsilon$ (solid line) and the contribution to I from the Mn site and the first shell of As neighbors (dotted line). Below E_F , the two lines are nearly coincident, showing that the magnetic moment is essentially confined to the Mn. At $E_F + \sim 0.25$ eV, there is approximately one electron difference in the “localized” and total DOS; this is the “delocalized” hole referred to in model descriptions. The *extent of localization* of eigenstates at E_F can be estimated from the *localized* DOS (slope of the dotted line) as a portion of *total* DOS (slope of the solid line). Evidently, a substantial portion of the weight is confined to Mn and its nearest neighbors. Thus, the t_{2g} state is best characterized as a deep level, though in the case of Mn:GaAs, it coincidentally falls near the valence-band edge. Wave functions at E_F are not effective-masslike but are a partially delocalized resonance of the impurity Mn d with the host. We conclude that the prospects of p type spin-polarized transport are intrinsically poor.

Turning to the case of magnetic “dimers” (pairs of dopants at nearest-neighbor cation sites), the localized majority t_{2g} levels now split into three bond-antibond pairs, two of them degenerate. The “dimer” amounts to an approximate realization of the classical two-centers tight-binding model introduced by Anderson and Hasegawa.⁷ Their model illus-

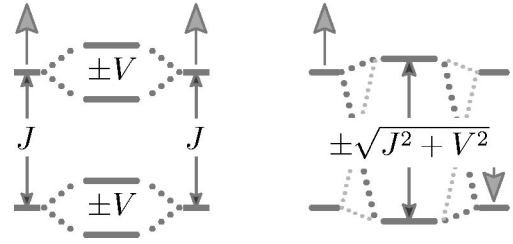


FIG. 3. Energy levels in the Anderson-Hasegawa two-centers hamiltonian. Left: the FM case ($\theta=0$). Levels of the same energy couple between sites, leading to energies $\pm V$. Right: the AFM case ($\theta=\pi$). Coupling is now between levels split by J , leading to energies $\pm \sqrt{J^2 + V^2}$.

trates qualitatively the competition between FM double-exchange (DEX) and AFM superexchange (SEX) interactions, and its dependence on filling. A pair of energy levels at each center are spin split by the internal magnetic field by $\pm J$, with the field at the second center canted by an angle θ . The levels are coupled to the other center (indirectly through the bonding to the host) by a hopping matrix element V (see Fig. 3). If $J \gg V$, the resulting eigenvalues may be expanded in V/Δ with $\Delta^2 = J^2 + V^2 \approx J^2$:

$$\epsilon = \mp \left[\Delta \pm \frac{VJ}{\Delta} \cos(\theta/2) - \frac{V^2 J^2}{2\Delta^3} \cos^2(\theta/2) + \dots \right]. \quad (1)$$








When an odd number of states are filled, the first (DEX) term dominates and the energy is minimized in the FM alignment ($\theta=0$). When an even number of states are filled, the DEX term vanishes and the system is stabilized in the AFM alignment ($\theta=\pi$) by the second (SEX) term. As the filling changes continuously there is a transition from FM stabilization to AFM. Detailed LDA calculations approximately confirm this picture.⁸ If the impurity is Mn (or Cr, or Fe) four (or two, or six) of the twelve t_{2g} states are filled. (The bonding e_g levels are always filled and add to the SEX term.) As the first column in Table I shows, Mn_2 , Cr_2 , and MnCr are strongly FM, while Fe_2 is strongly AFM for all the cases studied. Competition between FM and AFM interaction was also suggested by Akai⁹ on the basis of CPA calculations of the exchange interactions in the (InMnA)As alloy as a function of the n type dopant A (A=As or Sn). He found a transition from FM to antiferromagnetic (AFM) stabilization as a function of A concentration.

To further investigate the exchange interactions consider configurations more complex than dimers (see Table I). They show (i) the exchange J_{ij} connecting sites i and j depend sensitively on the lattice arrangement of impurities for a given doping level N_d ; (ii) an anomalous decrease in the effective J_{ij} as N_d increases (iii) large deviations from the pairwise Heisenberg form,

$$E = - \sum_{ij} J_{ij} \vec{s}_i \cdot \vec{s}_j. \quad (2)$$

Assuming that Eq. (2) is valid for some particular impurity configuration, we can extract the J_{ij} by computing the total energy E for a judicious choice of spin configurations

TABLE I. Heisenberg parameters (in meV) deduced from a Connolly-Williams prescription for various molecular clusters embedded in a 216-atom ZB host. Symbols $\uparrow\uparrow$, $\uparrow\uparrow\uparrow$, $\uparrow\uparrow\uparrow\uparrow$, and $\uparrow\uparrow\uparrow\uparrow\uparrow$ refer to clusters of 2, 3, 4 (tetrahedron) and 5 (pyramid) magnetic atoms. Also shown are figures depicting geometries of clusters. J_n refers to the Heisenberg interaction between n^{th} nearest neighbors entering into Eq. (2), deduced from a Connolly-Williams inversion. The J are defined with the convention $|\vec{s}_i| = 1$. In high symmetry cases, J reduces to 1/4 of the total energy difference between the FM state and a state with a single spin flipped. Quantities in parentheses include spin-orbit coupling, with a (001) spin quantization axis. “MnCr:GaN” denotes a cluster containing a single Cr.

	$\uparrow\uparrow$ 	$\uparrow\uparrow\uparrow^a$ 	$\uparrow\uparrow\uparrow\uparrow$ 	$\uparrow\uparrow\uparrow\uparrow\uparrow$ 			$\uparrow\uparrow^b$ 	$\uparrow\uparrow\uparrow^c$ 		$\uparrow\uparrow\uparrow^d$ 	
	J_1	J_1	J_1	J_1	J_1'	J_2	J_2	J_1	J_2	J_2	J_4
Mn:GaAs	55 (48)	41 (38)	24	14	30	-27	15 (11)	50	-11	9	20
Mn:GaN	78	45	20	-2	12	-54	23	47	-15	9	
Mn:AlN	51	10									
Fe:GaAs	-117	-115									
Fe:AlN	-170	-122									
Cr:GaAs	89 (88)	52 (52)									
MnCr:GaN	35	49	48								

^aNN Trimer.

^b2NN dimer: impurities at (0,0,0) and (0,0,1).

^cTrimer with two NN pairs and one 2NN pairs.

^dTrimer with two 2NN pairs and one 4NN pair.

with inequivalent combinations of pair correlation functions $\vec{s}_i \cdot \vec{s}_j$, which results in a set of linear equations for the J_{ij} . Table I shows parameters deduced in this way for a variety of magnetic clusters. The NN and 2NN pair parameters J_1 and J_2 decrease markedly with increasing cluster size—and consequently doping level since the magnetic and dopant atoms are the same here. For the pyramid, there are two inequivalent NN pairs (the apex-base and base-base pairs), which differ by a factor of two in GaAs, and in GaN the apex-base J_1 even changes sign. Table I reflects an apparently general tendency for the coupling to diminish in the presence of other nearby magnetic impurities. More distant impurities exert significantly less influence than ones nearby; for example, J_1 for the trimer with two NN and one 2NN pairs ($\uparrow\uparrow\uparrow$ in Table I) is closer to the dimer $J_1(\uparrow\uparrow)$ than to J_1 in the trimer with all NN pairs ($\uparrow\uparrow\uparrow$).

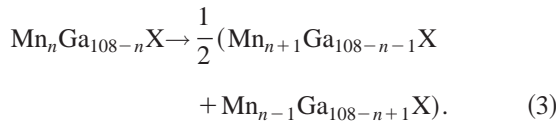
We must proceed to more complicated configurations to establish whether Eq. (2) itself is valid. In such cases, there are more inequivalent spin configurations than parameters J_{ij} , and the determination of J_{ij} is not unique. Four dopants arranged in a line along (1/2,1/2,0) has three exchange pa-

rameters but five possible spin configurations ($\uparrow\downarrow\downarrow\uparrow$, $\uparrow\uparrow\downarrow\downarrow$, $\uparrow\downarrow\downarrow\downarrow$, $\uparrow\downarrow\uparrow\downarrow$, and $\uparrow\downarrow\uparrow\uparrow$). A least squares fit to all five spin configurations results in $J_1 = 38$ meV, intermediate between the trimer and tetrahedron (see Table I). However, J_4 comes out -9 meV. If the first and last configurations are employed alone (they involve only J_1 and J_4), very different values of J_1 (23 meV) and J_4 (+9 meV) result.

The anomalies in J are striking when compared to RKKY-like theories, the conventional approach to modeling exchange in these compounds.² RKKY-like models predict that J_{ij} increases with concentration as $N_d^{1/3}$ at 0 K,³ and for fixed N_d are independent of environment. That the effective J are sensitive to environment and weaken with increasing concentration not only contradicts that theory, but suggests that the observed maximum in the critical temperature¹⁰ with increasing Mn concentration x may be an *intrinsic materials property*. With increasing concentration, the number of TM pairs increase, thus increasing T_c . But at larger concentrations, when defects are no longer well separated, the contribution *per pair* starts to decrease more rapidly, leading to a maximum in T_c . The perturbative RKKY model is in-

adequate to describe the exchange because the magnetic elements introduce large perturbations to the host, so that the resulting electronic structure and attendant quantities such as the magnetic susceptibility are dramatically altered.

We now turn to a discussion of the effective alloy Hamiltonian, i.e., how the *total* energy of the system depends on the configuration of magnetic TM impurities. Typically, the energy gained by bringing together two well-separated impurities in a dilute alloy is small and negative—on the order of -10 meV for alloys with lattice mismatches comparable to the (Mn,Ga) case. It is usually negative because it is dominated by the strain energy from the lattice mismatch. On this scale, the energy change in the Mn dimerization is of the opposite sign, and enormous. For example, the heat of reaction to dimerize two Mn atoms initially separated by $\sqrt{11}d$, ($d =$ “dimer” distance $= a/\sqrt{2}$, with a the lattice constant) was calculated to be $+181$ meV in GaAs, and $+640$ meV in GaN. The energy gain in forming a Mn “trimer” is larger still, showing that there is a strong driving force for the Mn to group into small nanoclusters. To estimate the lowest-energy cluster size, consider the reaction decomposing a pair of n atom clusters into a $n+1$ and a $n-1$ atom cluster:



The heat of this reaction is depicted in Fig. 4; the optimum cluster size n_{opt} corresponds to where the heat of reaction is ~ 0 . It is seen that $n_{opt} \approx 3$ for all the cases studied. (Figure 4 ignores entropy contributions to the free energy, $\Delta S \sim kT \Delta[(x/n) \log(x/n)]$, as they are negligible on the scale of Figure 4. For example, for $x=0.05$ and $n=3$, $\Delta S \sim kT/30$.) The strong pair interactions and the data in Fig. 4 show that, *in addition* to the NN pair interaction being anomalous, there are large three-body NN (and possibly other) contributions of the opposite sign, that combine to overtake the pair interactions for compact clusters where there are many such terms. Repeating the calculations *nonmagnetically* much smaller and of the opposite sign, as is typical in semiconductor alloys. This shows conclusively that the anomalous internuclear interaction arises from the magnetism.

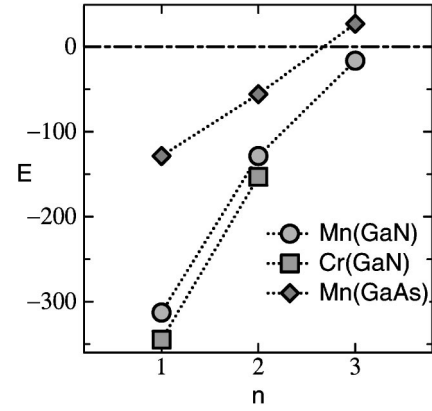


FIG. 4. Calculated heat of reaction, in meV, of two n atom clusters decomposing into an $n+1$ and an $n-1$ atom cluster. Data are for Mn in GaN (circles), Mn in GaAs (diamonds), and Cr in GaN (squares).

It is clear that because the (Mn,Ga)As alloy is grown at only ~ 250 C° to avoid phase segregation of MnAs into a NiAs phase, the tendency to clusterization may be kinetically limited. The kinetic considerations depend on growth conditions and are, in any case, difficult to model. We do not consider them further except to note that for GaN, the large N_2 binding energy requires that molecular beam epitaxy (MBE) growth occur under metastable conditions; thus, the kinetic effects may well be very different there than in GaAs.

The strong attraction between magnetic elements—unknown in ordinary semiconductor alloys—and the anomalies in the exchange interactions, are related. Both originate from the intra-atomic exchange being large in comparison to the bonding between d orbitals. Clearly, both must be taken into account to formulate an adequate theory of ferromagnetism in these materials.

In conclusion, we have shown that the magnetic TM doped III-V semiconductors form deep levels. They are responsible for magnetic exchange interactions that deviate strongly from simple model considerations, and also give rise to an anomalous contribution to the effective alloy Hamiltonian.

¹H. Ohno *et al.*, Appl. Phys. Lett. **69**, 363 (1996); H. Ohno *et al.*, Phys. Rev. Lett. **68**, 2664 (1992).

²T. Dietl, H. Ohno, F. Matsukura, J. Cibert, and D. Ferrand, Science **287**, 1019 (2000).

³T. Jungwirth, W.A. Atkinson, B.H. Lee, and A.H. MacDonald, Phys. Rev. B **59**, 981 (1999).

⁴O.K. Andersen, Phys. Rev. B **12**, 3060 (1975).

⁵P. Blochl, O. Jepsen, and O.K. Andersen, Phys. Rev. B **49**, 16 223 (1994).

⁶T. Kotani, J. Phys. Chem. **12**, 2413 (2000).

⁷P.W. Anderson and H. Hasegawa, Phys. Rev. **100**, 675 (1955); P. W. Anderson, in *Magnetism I*, edited by Rado and Suhl (Academic Press, New York and London, 1963).

⁸When the energy is computed as a function of θ , it does not follow the behavior $E(\theta) \propto |\cos(\theta/2)|$ expected from the Zener model, but is much closer to the Heisenberg $E(\theta) \propto |\cos(\theta)|$. This shows that the simple DEX/SEX model is only of limited validity here.

⁹H. Akai, Phys. Rev. Lett. **81**, 3002 (1998).

¹⁰H. Ohno, F. Matsukura, T. Omiya, and N. Akiba, J. Appl. Phys. **85**, 4277 (1999).